

FDP-6

Submitted 2 November 2009

Flux pinning properties of MgB₂ thin films on Ti buffered substrate prepared by
molecular beam epitaxy

K. Yonekura^{a*}, A. Kugo^a, T. Fujiyoshi^a, T. Sueyoshi^a, Y. Harada^b, M. Yoshizawa^c, T.
Ikeda^c, S. Awaji^d, K. Watanabe^d

^aDepartment of Computer Science and Electrical Engineering, Kumamoto University,
2-39-1, Kurokami, Kumamoto 860-8555, Japan

^bJST satellite Iwate, 3-35-2, Iiokashinden Morioka, Iwate 020-0852, Japan

^cDepartment of Materials Science and Engineering, Iwate University, 4-3-5, Ueda,
Morioka, Iwate 020-8551, Japan

^dInstitute for Materials Research, Tohoku University, 2-1-1, Katahira, Aoba-ku, Sendai
980-8577, Japan

Abstract

Transport properties of the MgB₂ thin films on Si, MgO and ZnO substrates with Ti buffer layer prepared by molecular beam epitaxy were investigated to clarify effects of the substrates and the Ti buffer layer on flux pinning. The critical current density J_c of each sample shows different dependence on magnetic fields parallel to c -axis. However, the scaling analysis of the macroscopic pinning force for all the measured samples implies that the grain boundaries work as the dominant pinning centers for $B//c$. The pinning parameter for MgB₂/Ti/Si estimated from the electric field E vs. the current density J characteristics shows the highest value among all the measured samples. This result is attributed to the high density of grain boundaries caused by the effect of both the Ti buffer and Si substrate in the growth process. Therefore, the selection of substrates and buffer layer strongly affects the flux pinning properties of MgB₂ thin films and plays an important role in the determination of performance for superconducting devices and wires.

Keyword: critical current density, Ti buffer layer, grain boundary

*Corresponding author

Kenji Yonekura

Postal address: Department of Computer Science and Electrical Engineering,

Kumamoto University, 2-39-1, Kurokami, Kumamoto 860-8555, Japan

Phone: +81 96 342 3640

Fax: +81 96 342 3630

E-mail address: kenji@st.cs.kumamoto-u.ac.jp (K. Yonekura)

Introduction

MgB₂ has the highest critical temperature T_c of 39 K among metallic superconductors [1]. This superconductor has some advantages which are usable in liquid hydrogen, a simple crystal structure, a low material cost and long coherence length. Therefore, MgB₂ superconductors are expected to be applied to various fields, such as wires and electronic devices.

High quality MgB₂ thin films are prepared by molecular beam epitaxy (MBE) [2] and electron beam evaporation (EBE) [3]. As-grown MgB₂ thin films deposited at low temperature by MBE and EBE have a high critical current density J_c . It is well known that dominant pinning centers of MgB₂ thin films on Al₂O₃ deposited by MBE and EBE are grain boundaries [4, 5]. The grain boundaries grow up perpendicular to surface in most cases. Then, the grain boundaries are effective pinning centers in magnetic field perpendicular to the surface. For this reason, MgB₂ thin films prepared by MBE and EBE show high critical current density J_c in the magnetic field perpendicular to the surface. However, further improvement of J_c in MgB₂ thin films are required for the high field application. Therefore, we need to introduce more effective pinning centers to MgB₂ thin films or to enhance pinning force of MgB₂ grain boundaries.

In this study, the MgB₂ thin films were prepared on various Ti buffered substrates.

In order to investigate influence of Ti buffer layer and substrates on flux pinning properties, we measured the magnetic field dependence of J_c , field angular dependence of J_c and the electric field E vs. current density J characteristics. The vortex glass-liquid transition temperature T_g and the pinning parameter m were estimated from $E - J$ characteristics. So, we can discuss the flux pinning properties of MgB₂ thin films on Ti buffered substrates in the viewpoint of the pinning strength distribution from the magnetic field dependence of m .

Experimental

MgB₂ thin films were deposited on MgO(100), Si(111) and ZnO(001) substrates with Ti buffer layer and MgO substrate without Ti buffer layer by MBE [6]. The substrates were set in the deposition chamber, and heated at 200 °C by tantalum heater. Base pressure of deposition chamber was very low about less or equal to 4×10^{-10} Torr. The evaporation sources were a pure magnesium block (99.99%) and stuffed granular boron (99.9%). The flux rate of B was 0.03 nm/s and the flux rate of Mg was from eight to nine-fold of that of B. The thicknesses of MgB₂ thin films are 150 nm (MgB₂/Ti/MgO, MgB₂/Ti/Si) and 300 nm (MgB₂/Ti/ZnO, MgB₂/MgO) respectively. The x-ray diffraction analysis shows that the all samples are oriented along c -axis. The

Ti buffer layer was deposited on a substrate before the deposition of MgB₂, and thicknesses of Ti buffer layers are 50 nm (MgB₂/Ti/MgO, MgB₂/Ti/Si) and 20 nm (MgB₂/Ti/ZnO), respectively. The Ti layer for protection was deposited on surface of MgB₂ thin films. The thickness of protection layer is about 3~5 nm. Table 1 summarizes the deposition parameters for each sample.

The lattice mismatching of MgB₂ for ZnO and Ti is small with 5.24% and 4.47%, respectively. On the other hand, the lattice mismatching of MgB₂ for MgO(100) and Si(111) are very large with 30.8% and 21.78%. However, it has been known that a 45° in-plane rotation of the MgB₂ lattice with MgO results in the lattice mismatching of only ~3% for two unit cells of MgB₂ on a MgO unit cell [7,8].

In order to measure the transport properties, the samples were patterned into a microbridge shape of 30 μm wide and 1 mm long by photolithography. To obtain good contact, Au contact pads were deposited on the films by RF sputtering after cleaning the film surfaces. The transport properties were measured by a four probe method. The magnetic field was applied by a 20 T superconducting magnet. The angle of external magnetic field was changed by rotating a sample holder in the superconducting magnet. The temperature was stabilized within ±0.03 K. The value of J_c was evaluated from the transport properties with the criterion of the electric field $E_c = 1 \mu\text{Vcm}^{-1}$. A magnetic

field angle is defined such that $B//c$ is $\theta = 0^\circ$ and transport currents are always perpendicular to the c -axis and the magnetic fields.

Results and discussion

Fig.1 shows the temperature dependence of resistivity ρ . $\text{MgB}_2/\text{Ti}/\text{MgO}$, $\text{MgB}_2/\text{Ti}/\text{Si}$, MgB_2/MgO and $\text{MgB}_2/\text{Ti}/\text{ZnO}$ have the critical temperatures T_c of 32.7 K, 34.3 K, 33.6 K and 34.9 K, respectively. The resistivity of $\text{MgB}_2/\text{Ti}/\text{Si}$ is highest among the all samples. The resistivity of $\text{MgB}_2/\text{Ti}/\text{Si}$ is about four times higher than the lowest resistivity of $\text{MgB}_2/\text{Ti}/\text{ZnO}$. Although $\text{MgB}_2/\text{Ti}/\text{MgO}$ and MgB_2/MgO are the same substrate, the resistivity of $\text{MgB}_2/\text{Ti}/\text{MgO}$ is higher than that of MgB_2/MgO .

The $B - T$ phase diagram is estimated from the $\rho - T$ curves in the magnetic fields. Fig. 2 shows the temperature dependence of upper critical current field B_{c2} and irreversibility field B_{irr} for $\text{MgB}_2/\text{Ti}/\text{MgO}$ and $\text{MgB}_2/\text{Ti}/\text{Si}$. The values of B_{c2} are defined as the mid points of resistivity ρ in the transition regions of $\rho - T$ curves up to 15 T. The $B_{\text{irr}}(T)$ curves are determined by the temperatures when the resistivity becomes 0.1% of resistivity immediately before the transition at each magnetic field. B_{c2} and B_{irr} of $\text{MgB}_2/\text{Ti}/\text{Si}$ are higher than those of $\text{MgB}_2/\text{Ti}/\text{MgO}$ in the high magnetic field. It is considered that the higher B_{c2} in $\text{MgB}_2/\text{Ti}/\text{Si}$ is due to the diffusion of Si into the MgB_2 thin film. This tendency was also reported by Harada *et al* [9]. We cannot confirm that

Si in the MgB₂ thin film becomes the impurity or the second phase material. However, it is considered that the highest resistivity of MgB₂/Ti/Si is caused by the diffusion of Si into the MgB₂ thin film.

Fig.3 shows the dependence of J_c on the magnetic fields applied in the direction parallel to the c -axis at 20 K. In the low magnetic fields, MgB₂/Ti/ZnO shows the highest J_c of all samples. In the magnetic fields from 3 T to 8 T, MgB₂/Ti/MgO shows the highest J_c and MgB₂/Ti/Si shows the highest J_c over 8 T. The value of J_c of MgB₂/Ti/MgO is higher than that of MgB₂/MgO in all magnetic fields.

Fig.4 shows the normalized macroscopic pinning force density, $f = F_p/F_{pmax}$, as a function of the normalized $b = B/B_{irr}$. The normalized pinning force density is fitted to the expression $f = Ab^p(1-b)^q$. In Fig.4, the solid line denotes in the case of $p = 0.9$ and $q = 2.1$. The data of the all samples is fitted to the solid line. When the dominant pinning centers are the grain boundaries, the parameters are $p = 0.5\sim 1.0$ and $q \approx 2.0$ [10,11]. Then the effective pinning centers of all samples would be grain boundaries.

Fig.5 shows the field angular dependence of J_c at 20 K for 3 T. Then a large peak at $\theta = 0^\circ$ appears in the all samples. This result indicates that the all samples have c -axis correlated pinning centers which are grain boundaries as mentioned above. The value of J_c of MgB₂/Ti/MgO is higher than that of MgB₂/MgO in all angles in spite of the same

substrate. Small peaks at $\theta = 90^\circ$ are due to the intrinsic pinning of MgB_2 .

Although the grain boundaries act as dominant pinning centers in all samples, there is a difference in the J_c . The highest J_c in the low magnetic fields was observed in $\text{MgB}_2/\text{Ti}/\text{ZnO}$. This result would be caused by the low density of grain boundaries, which means that $\text{MgB}_2/\text{Ti}/\text{ZnO}$ has large MgB_2 grains. The large MgB_2 grains originate from a little lattice mismatching between MgB_2 and Ti buffered $\text{ZnO}(001)$ substrate. The highest J_c was observed in $\text{MgB}_2/\text{Ti}/\text{MgO}$ from 3 to 8 T. This result indicates the higher density of grain boundaries. The high density of grain boundaries is caused by small MgB_2 grains. It is considered that the higher density of grain boundaries is caused by the effect of both Ti buffer layer and MgO substrate in growth process. Furthermore, $\text{MgB}_2/\text{Ti}/\text{Si}$ shows the highest J_c above 8T. Then it is predicted that the density of grain boundaries in $\text{MgB}_2/\text{Ti}/\text{Si}$ would be higher than that in $\text{MgB}_2/\text{Ti}/\text{MgO}$. In addition, it was reported that the small MgB_2 grains cause high B_{c2} [12]. Therefore, the high B_{c2} for $\text{MgB}_2/\text{Ti}/\text{Si}$ may be due to both the diffusion of Si into the MgB_2 thin film and small MgB_2 grains.

The isothermal $E - J$ curves of $\text{MgB}_2/\text{Ti}/\text{MgO}$ at 1 T for $B//c$ are shown in Fig.6. The $E - J$ curves at a low temperature region have negative curvatures in a log-log plot. As the temperature increases, the $E - J$ curves vary from a negative curvature to a positive

curvature on reaching a certain temperature. This temperature is called the glass-liquid transition temperature T_g . It has been reported that the $E - J$ characteristics of high- T_c superconductors are expressed by the percolation transition model. According to this model [13], the probability function of local current density J_{cl} is given by the Weibull distribution function as

$$P(J_{cl}) = \left(\frac{J_{cl} - J_{cm}}{\Delta J_c} \right)^{m-1} \exp \left[- \left(\frac{J_{cl} - J_{cm}}{\Delta J_c} \right)^m \right], \quad (1)$$

where J_{cm} is the minimum value of the distribution of the local current density, ΔJ_c is the half width of the distribution, and m is the pinning parameter which characterizes the shape of the distribution function. When the distribution of pinning strength is more uniform, the value of the pinning parameter m becomes larger. Using the distribution function Eq. (1), the $E - J$ characteristics are given as follow:

$$E = \rho_{FF} \int_{J_{cm}}^J (J - J_{cl}) P(J_{cl}) dJ_{cl} = \begin{cases} \frac{\rho_{FF} \Delta J_c}{m+1} \left(\frac{J - J_{cm}}{\Delta J_c} \right)^{m+1} & \text{for } T < T_g \\ \frac{\rho_{FF} \Delta J_c}{m+1} \left(\frac{J}{\Delta J_c} \right)^{m+1} & \text{for } T = T_g \\ \frac{\rho_{FF} \Delta J_c}{m+1} \left\{ \left(\frac{J + |J_{cm}|}{\Delta J_c} \right)^{m+1} - \left(\frac{|J_{cm}|}{\Delta J_c} \right)^{m+1} \right\} & \text{for } T > T_g \end{cases} \quad (2)$$

where ρ_{FF} is the flux flow resistivity. We fitted the theoretical expression Eq. (2) to the $E - J$ curves of MgB₂ thin films. The pinning parameters J_{cm} , ΔJ_c and m were determined as the error between experimental data and fitting theoretical curves makes minimum.

As shown in Fig.6, the theoretical curves are in excellent agreement with the experimental data in all measured temperatures. In the same way, the theoretical curves are in good agreement with the experimental data of MgB₂/Ti/Si and MgB₂/MgO.

Fig.7 shows the magnetic field dependence of m for MgB₂/Ti/MgO, MgB₂/Ti/Si and MgB₂/MgO. In all magnetic fields, MgB₂/Ti/Si shows the highest m -values. This result indicates that the distribution of pinning strength is very uniform. The high m value probably originates from the high density of grain boundaries in MgB₂/Ti/Si. This result coincides with the magnetic field dependence of J_c . The value of m of MgB₂/Ti/MgO is higher than that of MgB₂/MgO. This result indicates that the density of grain boundaries is higher than that of MgB₂/MgO.

Conclusions

In this study, we deposited MgB₂ thin films on Ti buffered substrates. In order to investigate the effects of various substrates and Ti buffer layer, the temperature dependence of resistivity in the magnetic field, the magnetic field dependence of J_c , field angular dependence of J_c , and $E - J$ characteristics were measured. In the $B - T$ phase diagram, MgB₂/Ti/Si shows the high B_{c2} at low temperature. MgB₂/Ti/ZnO shows the highest J_c in the low magnetic fields, MgB₂/Ti/MgO shows the highest J_c from 3 to 8 T and MgB₂/Ti/Si shows the highest J_c above 8 T, respectively. The scaling analysis of

the macroscopic pinning force density shows that the grain boundaries are the dominant pinning centers in all samples. It is confirmed that the all samples have the c -axis correlated pinning centers due to the grain boundaries from the field angular dependence of J_c . The highest J_c of $\text{MgB}_2/\text{Ti}/\text{ZnO}$ in the low magnetic field originates from the low density of grain boundaries by a little lattice mismatching between MgB_2 and the Ti buffered $\text{ZnO}(001)$ substrate. On the other hand, The highest J_c of $\text{MgB}_2/\text{Ti}/\text{MgO}$ in 3 to 8 T is due to the high density of grain boundaries by the effect of both Ti buffer layer and $\text{MgO}(100)$ substrate. The highest value of J_c of $\text{MgB}_2/\text{Ti}/\text{Si}$ over 8 T is caused by the high density of grain boundaries and its high B_{c2} . This result coincides with the highest m -value of $\text{MgB}_2/\text{Ti}/\text{Si}$. Therefore, $\text{MgB}_2/\text{Ti}/\text{Si}$ has a uniform distribution of pinning strength.

Therefore, we can control the density of grain boundaries in MgB_2 thin films using the various substrates and Ti buffer. This method is useful for the application of electronic devices and wires since the value of J_c changes with grain size.

References

- [1] J. Nagamatsu, N. Nakagawa, T. Muranaka, Y. Zenitani, J. Akimatsu, *Nature* 410 (2001) 63.
- [2] M. Haruta, T. Fujiyoshi, S. Kihara, T. Sueyoshi, K. Miyahara, Y. Harada, M. Yoshizawa, T. Takahashi, H. Iriuda, T. Oba, S. Awaji, K. Watanebe, R. Miyagawa, *Supercond. Sci. Technol.* 20 (2007) 1.
- [3] M. Okuzono, T. Doi, Y. Ishizaki, Y. Kobayashi, Y. Hakuraku, H. Kitaguchi, *IEEE Trans. Appl. Supercond.* 15 (2005) 3253.
- [4] A. Saito, H. Shimakage, A. Kawakami, Z. Wang, K. Kuroda, H. Abe, M. Naito, W. J. Moon, K. Kaneko, M. Mukaida, S. Ohshima, *Physica C* 412-414 (2004) 1366.
- [5] H. Kitaguchi, A. Matsumoto, H. Kumakura, T. Doi, H. Yamamoto, K. Saitoh, H. Sosiati, S. Hata, *Appl. Phys. Lett.* 85 (2004) 2842.
- [6] T. Takahashi, Y. Harada, H. Iriuda, M. Kuroha, T. Oba, M. Seki, Y. Nakanishi, J. Echigoya, M. Yoshizawa, *Physica C* 445-448 (2006) 887.
- [7] A. J. M. v. Erven, T. H. Kim, M. Muenzenberg, J. S. Moodera, *Appl. Phys. Lett.* 81 (2002) 4982.
- [8] S. D. Bu, D. M. Kim, J. H. Choi, J. Giencke, E. E. Hellstrom, D. C. Larbalestier, S.

Patnaik, L. Cooley, C. B. Eom, J. Lettieri, D. G. Schlom, W. Tian, X. Q. Pan, Appl.

Phys. Lett. 81 (2002) 1851.

[9] Y. Harada, T. Takahashi, M. Kuroha, H. Iriuda, Y. Nakanishi, F. Izumida, H. Endo,

M. Yoshizawa, Physica C 445 (2006) 884.

[10] D. Dew-Hughes, Cryogenics 15 (1975) 435.

[11] R. E. Enstrom, J. R. Appert, J. Appl. Phys. 43 (1972) 1915.

[12] A. Matsumoto, H. Kumakura, H. Kitaguchi, B. J. Senkowicz, M. C. Jewell, E. E.

Hellstorm, Y. Zhu, P. M. Voyles, D. C. Larbalestier, Appl. Phys. Lett. 89 (2006)

132508.

[13] K. Yamafuji, T. Kiss, Physica C 258 (1996) 197.

	MgB ₂ /Ti/MgO	MgB ₂ /Ti/Si	MgB ₂ /MgO	MgB ₂ /Ti/ZnO
substrate	MgO(100)	Si(111)	MgO(100)	ZnO(001)
buffer layer	Ti(50nm)	Ti(50nm)	none	Ti(20nm)
thickness	150nm	150nm	300nm	300nm

Table 1 Samples in this study

Figure captions

Fig.1 Temperature dependence of resistivity.

Fig.2 $B - T$ phase diagram.

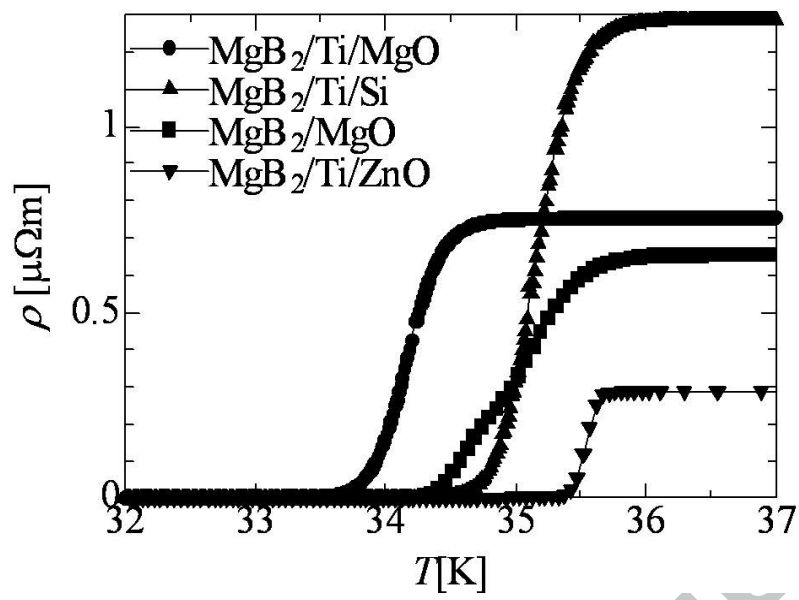
Fig.3 Magnetic field dependence of J_c at 20 K for $B//c$.

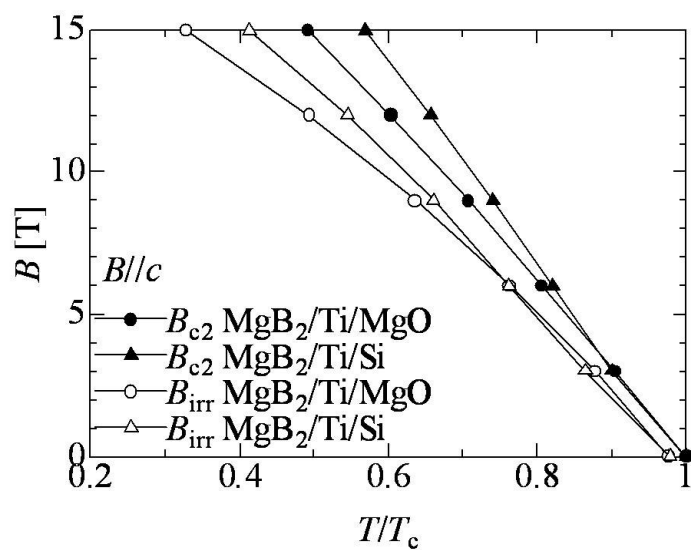
Fig.4 Scaling analysis of $F_p - B$ at 20 K for $B//c$.

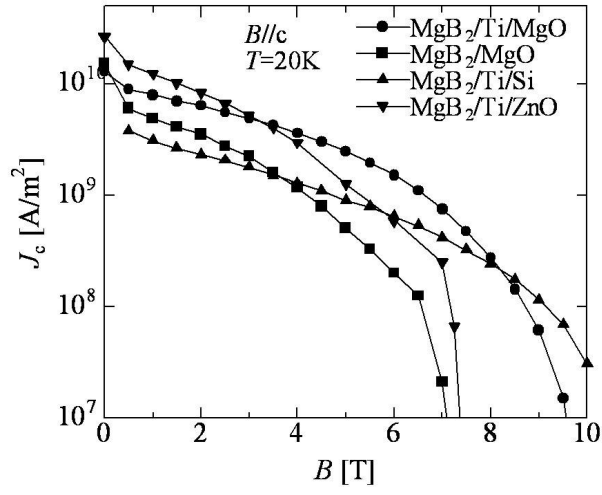
Fig.5 Field angular dependence of J_c at 20 K for 3 T.

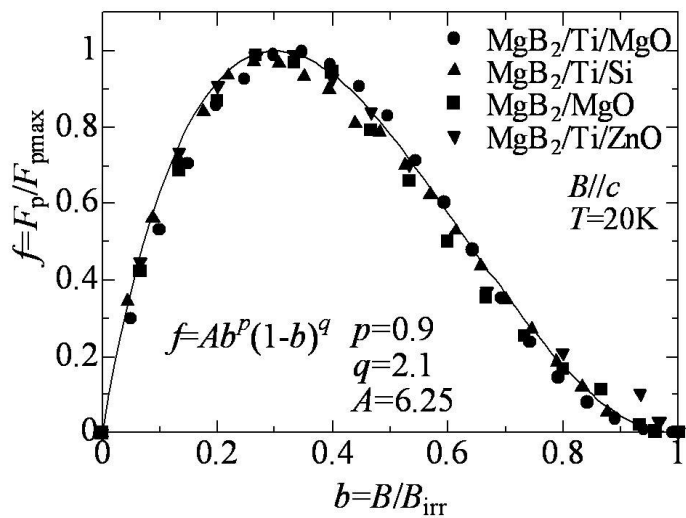
Fig.6 $E - J$ characteristics for $MgB_2/Ti/MgO$ at 1 T.

Fig.7 Magnetic field dependence of m at $B//c$.

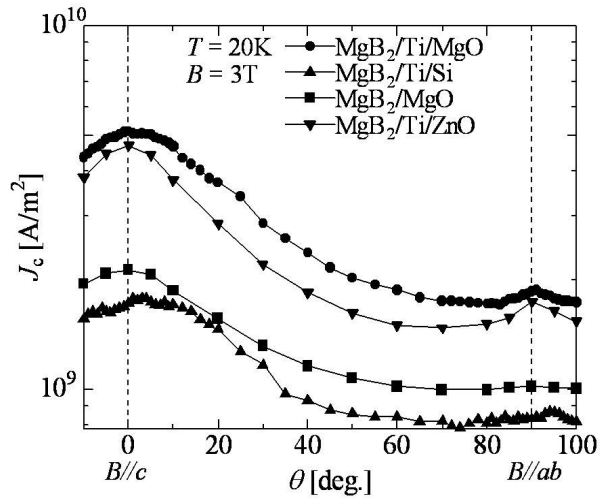




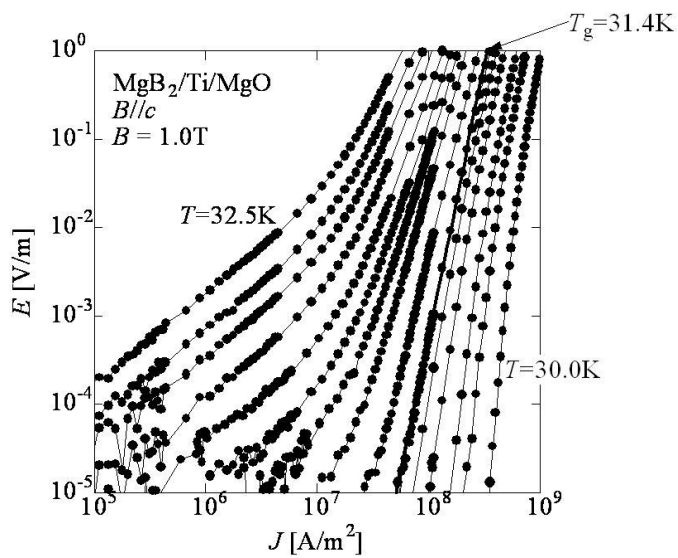


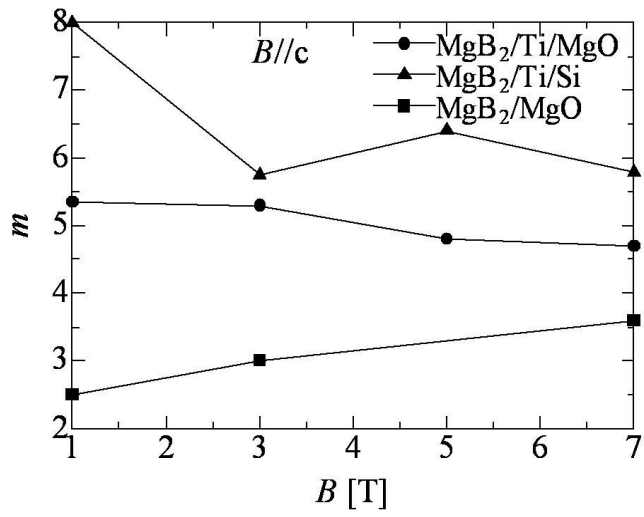


ACCEPTED MANUSCRIPT



ACCEPTED MANUSCRIPT





ACCEPTED MANUSCRIPT